REGULAR ARTICLE

blood advances

Development of a carotid artery thrombolysis stroke model in mice

Jessica A. A. Maclean,[1,2,*] Amelia J. Tomkins,[1,2,*] Sharelle A. Sturgeon,[1] Benjamin R. Hofma,[1,2] Imala Alwis,[1,2] Andre L. Samson,[1,2] Simone M. Schoenwaelder,[1,2,*] and Shaun P. Jackson[1-3,*]

[1]Heart Research Institute, Newtown, NSW, Australia; [2]Charles Perkins Centre, The University of Sydney, Sydney, NSW, Australia; and [3]Department of Molecular Medicine, The Scripps Research Institute, La Jolla, CA

Key Points

- Development of a mouse carotid artery thrombolysis model of stroke.
- iCAT enables assessment of adjunctive antithrombotic therapies on arterial recanalization, cerebral perfusion, and stroke outcomes.

Recanalization with restored cerebral perfusion is the primary goal of thrombolytic therapy in acute ischemic stroke. The identification of adjunctive therapies that can be safely used to enhance thrombolysis in stroke remains an elusive goal. We report here the development of a mouse in situ carotid artery thrombolysis (iCAT) stroke model involving graded cerebral ischemia to induce unihemispheric infarction after thrombotic occlusion of the common carotid artery (CCA). Electrolytic-induced thrombotic occlusion of the left CCA enabled real-time assessment of recanalization and rethrombosis events after thrombolysis with recombinant tissue-type plasminogen activator (rtPA). Concurrent transient stenosis of the right CCA induced unihemispheric hypoperfusion and infarction in the left middle cerebral artery territory. Real-time assessment of thrombolysis revealed recanalization rates <30% in rtPA-treated animals with high rates of rethrombosis. Addition of the direct thrombin inhibitor argatroban increased recanalization rates to 50% and reduced rethrombosis. Paradoxically, this was associated with increased cerebral ischemia and stroke-related mortality (25%-42%). Serial analysis of carotid and cerebral blood flow showed that coadministration of argatroban with rtPA resulted in a marked increase in carotid artery embolization, leading to distal obstruction of the middle cerebral artery. Real-time imaging of carotid thrombi revealed that adjunctive anticoagulation destabilized platelet-rich thrombi at the vessel wall, leading to dislodgement of large platelet emboli. These studies confirm the benefits of anticoagulants in enhancing thrombolysis and large artery recanalization; however, at high levels of anticoagulation (~3-fold prolongation of activated partial thromboplastin time), this effect is offset by increased incidence of carotid artery embolization and distal middle cerebral artery occlusion. The iCAT stroke model should provide important new insight into the effects of adjunctive antithrombotic agents on real-time thrombus dynamics during thrombolysis and their correlation with stroke outcomes.

Submitted 25 August 2021; accepted 21 June 2022; prepublished online on *Blood Advances* First Edition 29 June 2022; final version published online 23 September 2022. DOI 10.1182/bloodadvances.2021006008.

*J.A.A.M., A.J.T., S.M.S., and S.P.J. contributed equally to this study.

As per journal policy, the authors declare that all methodologies and supporting data are available within the article and supporting supplemental Data files, with relevant literature referenced. Additional protocol information is available from the corresponding authors upon reasonable request. Requests relating to the manuscript may be made by contacting simone.schoenwaelder@hri.org.

The full-text version of this article contains a data supplement.

Introduction

Thrombolytic therapy with recombinant tissue-type plasminogen activator (rtPA) is the only approved pharmacologic approach to achieve rapid vessel recanalization in acute ischemic stroke. rtPA-mediated thrombolysis facilitates large artery recanalization and improves clinical outcomes,[1,2] although its efficacy is limited by a time-constrained therapeutic window (rtPA must be given within 4.5 hours of stroke symptom onset). Other limitations include incomplete recanalization in up to 50% of treated patients and rethrombosis of successfully thrombolysed arteries in 14% to 34% of individuals.[3] rtPA therapy is also associated with a 4% to 8% incidence of symptomatic intracerebral hemorrhage (ICH).[3-5] As a result, the percentage of stroke patients who achieve clinical benefit from thrombolytic therapy is low (<10%).

Adjunctive antithrombotic therapies, including heparin and aspirin, have an important role in enhancing rtPA-mediated thrombolysis and preventing rethrombosis.[6] This has been most clearly shown in the acute coronary syndromes.[6-8] However, in ischemic stroke, anticoagulants and antiplatelet agents combined with rtPA increase the risk of symptomatic ICH and worsen patient outcomes.[9,10] Ongoing clinical trials are evaluating potentially safer adjunctive antithrombotic therapies for the hyperacute treatment of ischemic stroke. These include anticoagulant agents with an improved bleeding profile, such as the direct thrombin inhibitor argatroban, or antiplatelet agents such as Revacept (advanceCOR GmbH, Martinsried, Germany) or ACT017, that reduce collagen activation of platelets.[11] Argatroban provides an attractive option for adjuvant therapy, as preclinical studies have shown that argatroban reduces cerebral infarction after middle cerebral artery (MCA) occlusion (MCAO) when used in combination with rtPA.[12,13] Thrombin inhibitors have the potential to enhance recanalization and improve cerebral perfusion, partly by reducing the formation of microvascular thrombi.[12,14] Clinically, the ARTSS-2 (Randomized Controlled Trial of Argatroban With Tissue Plasminogen Activator [tPA] for Acute Stroke) trial reported excellent outcomes when rtPA was combined with argatroban,[11] although in humans it is unclear whether these benefits are primarily related to improved recanalization, microvascular perfusion, or a combination of both.

Insight into the ability of antithrombotic agents to enhance thrombolysis, large-artery recanalization, and restore cerebral perfusion would be facilitated by the development of an experimental mouse model that enables simultaneous assessment of these events. Although murine stroke models continue to play an important role in the understanding of stroke pathogenesis, they have limitations in their ability to assess adjunctive thrombolytic therapies. These limitations include difficulties assessing recanalization in intracranial vessels, susceptibility of thrombi to endogenous fibrinolysis,[15,16] or lack of thrombus for assessment, as in the intraluminal filament model of transient MCAO (tMCAO).[17] Models such as the embolic stroke model commonly rely on injection of ex vivo clots.[18-21] The intracranial injection of these clots requires monitoring of cerebral perfusion or assessment of kinetic changes of contrast dyes to assess recanalization events.[9,14-16] Other models initiate in vivo thrombus formation through photochemical or biochemical injury to the distal MCA and cerebral cortex, respectively,[22,23] or via thrombin injection into the bifurcation of the MCA to generate cortical infarction.[16] These models often require craniectomy, which can induce cerebral inflammation and changes to intracranial pressure or local cerebral temperature,[24] ultimately affecting stroke outcome.

The development of a mouse stroke model in which thrombotic occlusion of extracranial vessels is coupled with the real-time assessment of thrombolysis and cerebral perfusion, under experimental conditions leading to reproducible cerebral infarction, has represented a significant technical challenge. As such, there are currently no experimental models in which extracranial thrombotic occlusion of the carotid artery can be reliably coupled to a model of graded cerebral ischemia, leading to the generation of reproducible unihemispheric infarcts. This is primarily due to the variable nature of the mouse collateral blood supply and anatomical variations in the circle of Willis, such that unilateral occlusion of the extracranial carotid artery produces unreliable cerebral hypoperfusion in the ipsilateral hemisphere.

Here we present the development of the in situ carotid artery thrombolysis stroke model (termed iCAT) involving electrolytic-mediated thrombotic occlusion of the left common carotid artery (CCA) that is amenable to pharmacologic thrombolysis and the assessment of adjunctive antithrombotic agents. Combining unilateral CCA thrombotic occlusion with graded titration of blood flow through the contralateral (right) CCA, we have been able to reproducibly induce controlled depression of ipsilateral cerebral perfusion leading to focal cerebral ischemia and infarction. We found that serial analysis of cortical perfusion is predictive of infarct development and stroke outcomes. Moreover, the ability to concurrently monitor large artery recanalization and cerebral perfusion throughout stroke development helps elucidate the benefits and limitations of adjunctive thrombolytic therapies on cerebral blood flow (CBF) and stroke progression. Our studies confirm the ability of anticoagulants to enhance large artery recanalization when combined with rtPA; however, at high levels of anticoagulation, this increases the propensity to destabilize platelet thrombi and induce embolization.

Methods

A comprehensive description of additional methodology is available in the supplemental Data.

Animals

C57Bl/6J mice were purchased from Australian BioResources (Moss Vale, NSW, Australia) and housed at the Laboratory Animal Services facility (University of Sydney, Sydney, NSW, Australia), the PC2 Rodent Holding Facility (Heart Research Institute), and the Precinct Animal center (Baker Institute) Alfred Medical Research and Education precinct (Melbourne, VIC, Australia). All animals were housed in a 12-hour light/dark cycle with access to food and water ad libitum. For all studies, male mice aged between 8 and 12 weeks (20-30 g) were used.

All studies were approved by the Alfred Medical Research and Education precinct Animal Ethics Committee (E/1247/2012/M), the University of Sydney Animal Ethics Committee (2014/647; 2018/1343; 2018/1331), and the Sydney Local Health District Animal Welfare Committee (2020-012) in accordance with the requirements of the Australian Code of Practice for the Care and Use of Animals for Scientific Purposes.[25]

Surgical procedures and postoperative recovery

1. *Surgical preparation:* A complete and detailed description of methods adopted for surgical preparation is available in the supplemental Data.
2. *Thrombotic occlusion of the carotid artery and stroke induction:* Thrombosis of the left CCA was induced with electrolytic injury, as described previously[26-29] (supplemental Figures 1 and 2). The electrode was standardized and manufactured commercially by Ugo Basile (Comerio, VA, Italy); it comprised 2 platinum arms, each terminating in a small hook, both stabilized in place with insulated coating to prevent any increase in inter-arm distance over time, ensuring delivery of a uniform injury. To administer the electrolytic injury, the left CCA was gently placed in the crook of the hook-shaped electrode and the artery clamped distally to induce stasis (Micro Serrefine Clamp, 18055-05; Fine Science Tools, North Vancouver, BC, Canada). An electrical current (8 mA) was delivered continuously for 3 minutes through the platinum electrode using a lesion-making device (Model 53500; Ugo Basile) (supplemental Figure 1), while the site was constantly flushed with saline for the duration to enable efficient conduction of current to the vessel. Immediately after injury, the clamp was released, the flow probe replaced, and blood flow monitored for occlusion (defined as flow of 0 mL/min per 100 g).
3. *Stroke induction:* After 10 minutes of CCA occlusion, ligature-induced stenosis of the right (contralateral) CCA was commenced to reduce ipsilateral perfusion $<25\%$ of baseline, while maintaining contralateral perfusion $>25\%$ of baseline for the duration of ischemia (25, 45, and 60 minutes). Regional cerebral perfusion was continuously monitored with laser Doppler flowmetry (LDF) (supplemental Figure 1C). After ischemia, the ligature was removed to restore maximal blood flow through the contralateral CCA, and animals were recovered to 24 hours' postocclusion and assessed for cerebral infarction and functional outcomes (supplemental Figures 1 and 2).
4. *Cerebral Perfusion Monitoring:* Cerebral perfusion monitoring was conducted with laser speckle contrast imaging (LSCI) and LDF through the mouse skull. LSCI of cerebral perfusion (designated flux units) was obtained by using a moorFLPI-2 blood flow imager and associated software (moorFLPI-2 Measurement V1.1, Moor Instruments, Oxford, UK). For perfusion monitoring during surgical procedures, LDF was used as previously described with modifications.[19] Further details are supplied in the supplemental Data.
5. *Delivery of thrombolytic and adjunctive therapies*: Mice were randomly allocated to treatment, with the operator blinded to treatment allocation. In addition, animals within each cage were randomized to different treatment groups or procedures (ie, sham and stroke) to minimize cage effects on study outcomes. Thrombolytic and adjunctive therapies were delivered IV via the jugular vein, 15 to 20 minutes after stable CCA occlusion, unless stated otherwise (supplemental Figures 1 and 2). rtPA was purchased from Boehringer Ingelheim Pty Ltd (Actilyse, Alteplase; North Ryde, NSW, Australia) and dialyzed to remove arginine components, as described in detail in the supplemental Data and previously published data.[30] Thrombolytic therapy (rtPA, 10 mg/kg; 10% bolus with remainder infused over 30 minutes) was delivered IV alone or in combination with anticoagulant argatroban (bolus 80 μg/kg; infusion 40 μg/kg per minute over 60 minutes). Dose of argatroban was selected to elevate activated partial thromboplastin time (APTT) to 2- to 3-fold baseline values, in which the mean APTT at 15 minutes after IV delivery was 2.9-fold baseline values (range, 2.3- to 3.9-fold baseline; $n = 5$). To maintain overnight anticoagulation, ALZET Minipumps (Model 2001D; catalog no. 2001D0000294 [ALZ], BioScientific Pty Ltd., Kirrawee, NSW, Australia) were loaded with freshly prepared argatroban and aseptically implanted subcutaneously between the mouse scapulae to maintain a dose of 40 μg/kg per minute for the duration of recovery. The minipump was inserted in accordance with the manufacturer's recommendations.
6. *Postoperative recovery and temperature regulation:* A detailed description of methods adopted for postoperative recovery and temperature regulation is available in supplemental Data.

Real-time imaging of mouse thrombi with carotid artery transilluminator

To visualize thrombus formation and thrombolysis, the mouse carotid artery transilluminator[31,32] was positioned under the mouse carotid artery distal to the flow probe, so the carotid artery was illuminated from beneath the vessel. The transilluminator light guide was prepared from a clear acrylic rod (6-mm diameter, 5-cm length) attached to a 0.4-mm thick clear polycarbonate plastic strip (6-mm wide at the input end, 50-mm long, and 1.5-mm wide at the output end). The output end of the transilluminator was beveled (30-45 degrees) with a scalpel and bent at 4 mm to allow positioning of the transilluminator under the carotid artery. The whole transilluminator was wrapped in reflective tape (850 Polyester film tape; 3M, St. Paul, MN) and the tip subsequently wrapped in black photographic tape (Shurtape Technologies, Hickory, NC) to reduce light loss. The transilluminator was connected to a single flexible Schott surgical light guide (KL 1600 LED; Schott AG, Mainz, Germany) and secured in position with a retort stand. Real-time imaging of thrombus formation and thrombolysis was captured with a TrueChrome IIS (Tucsen Photonics, Fuzhou, China) camera attached to a Nikon SMZ745T surgical microscope. Imaging commenced at the time of treatment onset, or as described in the relevant figure legends, at a capture rate of 25 fps for 60 minutes after treatment onset.

Imaging of cerebral thrombi

Platelets were labeled with DyLight 488 anti-glycoprotein 1b antibody (X488; emfret Analytics, Würzburg, Germany; 100 μg/kg) before electrolytic injury of the mouse carotid artery. Ninety minutes after thrombotic occlusion, the brain was excised to visualize cerebral platelet deposition. The excised brain was imaged on a Nikon AZ100 Multizoom Macroscope fitted with AZ Plan Apo 1× NA 0.1 and AZ Plan Apo 4× NA 0.4 objectives (Nikon Instruments Inc., Tokyo, Japan), equipped with a CoolLED pE-300 Ultra-light source (CoolLED, Andover, United Kingdom), Semrock BrightLine LED-DA/FI/TR/Cy5-4X-B-NTE filter set (Semrock, West Henrietta, NY), and an Andor Sona sCMOS 4.2b camera (SONA-4BV6U Andor Technology, Belfast, United Kingdom), operated by Nikon NIS-Elements AR software (version 5.30.05; Nikon Instruments Inc.). Postimaging processing was performed by using Nikon NIS-Element's Clarify.ai algorithm module. Confocal imaging (20IMM objective x NA 0.7) of platelet emboli was performed by using a Leica SP8 (Wetzlar, Germany) confocal system and the three-dimensional data set acquired using LAS X version 3.5.7 (Leica Microsystems, Buffalo

Grove, IL). Three-dimensional data were rendered by using Imaris version 9.8 (Bitplane AG, Switzerland).

Data presentation and analysis

Statistical analysis was performed with GraphPad Prism version 8 (GraphPad Software, La Jolla, CA) or IBM SPSS Statistics version 26 (IBM Corporation, Armonk, NY) software packages. Statistical significance was assessed by using the appropriate statistical test as dictated by each individual data set, including (where indicated) the unpaired *t* test, Mann-Whitney test (for nonparametric distribution), ordinary one-way analysis of variance (corrected for multiple comparisons using one of Tukey, Dunnett's, or Šidák tests, where indicated), χ^2 test, or Fisher's exact test. The number of independent experiments is stated in the figure legends, and statistical significance is determined by *P* value, where $^{ns}P > .05$, $^{*}P < .05$, $^{**}P < .01$, $^{***}P < .001$, and $^{****}P < .0001$.

Results

Unilateral carotid artery occlusion inconsistently produces cerebral infarction

Restoration of arterial blood flow is the primary objective of thrombolytic therapy in stroke. Currently, there are no mouse stroke models involving extracranial thrombotic occlusion that allow assessment of the impact of thrombolytic therapies on large vessel recanalization and cerebral perfusion. We initially investigated the impact of unilateral carotid artery occlusion on cerebral infarction in the mouse. Electrolytic thrombotic occlusion of the ipsilateral CCA did not induce consistent cerebral infarction, with only 50% of animals presenting with 2,3,5-triphenyltetrazolium chloride (*TTC*)-delineated infarct at 24 hours (n = 6). Mean infarct volume was typically small after unilateral occlusion and predominately located within the hippocampal regions of the brain (supplemental Figure 3A). The absence of lesions or small lesions produced by unilateral carotid artery occlusion was unlikely to be a result of spontaneous carotid recanalization leading to incomplete hypoperfusion, as permanent carotid ligation also failed to produce consistent cerebral infarction. LDF analysis over the MCA territory confirmed that carotid artery thrombotic occlusion resulted in variable hypoperfusion within the ipsilateral hemisphere. Importantly, mice with sustained ipsilateral hypoperfusion (<30% of baseline perfusion) presented with small hippocampal infarcts at 24 hours (n = 3 of 6) (supplemental Figure 3B). In contrast, mice with sustained perfusion in the MCA territory (>30% of baseline) had no evidence of cerebral infarction at 24 hours.

Global cerebral hypoperfusion and infarction results in a high mortality rate

Natural variations in the vascular architecture of the mouse circle of Willis, particularly related to the posterior communicating artery, are likely to contribute to the variations in ipsilateral hypoperfusion induced by unilateral carotid artery occlusion. To circumvent this, we combined electrolytic-induced thrombotic occlusion of the ipsilateral (left) CCA with transient mechanical occlusion of the contralateral (right) CCA (thrombotic bilateral CCA occlusion) (supplemental Figure 1B) to reduce cerebral perfusion to a level necessary for the induction of neuronal death. The resultant transient global ischemia was sufficient to induce global hypoperfusion within the MCA territory, resulting in the development of small cerebral infarcts at 24 hours (supplemental Figure 3C-D). The extent of cerebral infarction correlated with the duration of ischemia (supplemental Figure 3D). We restricted global ischemia to 25 minutes, as prolonged ischemia (≥30 minutes) was associated with a high mortality rate (20% mortality rate at 25 minutes vs 61.5% at 30 minutes). With global ischemia, 68.4% (n = 13 of 19) of surviving mice displaying evidence of infarction at 24 hours. Bilateral hypoperfusion ≥80% reduction from baseline perfusion was predictive of stroke-related mortality, cerebral infarction, and functional deficits (supplemental Figure 3E). Induction of severe global ischemia (LDF ≥ 90% of baseline in both hemispheres) was poorly tolerated, resulting in rapid death in 21% of mice (n = 10 of 47; mean ± SD time to death, 12.12 ± 4.09 minutes).

Graded ischemia leads to reproducible unilateral hypoperfusion and cerebral infarction

Given the variable infarction with global hypoperfusion and the relatively high mortality rate, we examined the feasibility of combining thrombotic occlusion of the left CCA with controlled stenosis of the right contralateral CCA, with the aim of producing left ipsilateral cerebral hypoperfusion and focal ischemia (supplemental Figures 1C and 2). To depress ipsilateral cerebral perfusion, we used a silk suture to transiently stenose the contralateral right CCA until CBF in the left (ipsilateral) hemisphere was <25% baseline (mean ± SD, 14.19% ± 5.34%; n = 25) (Figure 1A). Compared with the global CBF depression observed with the thrombotic bilateral common carotid artery occlusion procedure, stenosis of the right CCA ensured that average CBF in the contralateral hemisphere remained above the ischemic threshold for the duration of the 60-minute stenosis period (mean ± SD, 84.13 ± 27.16%; n = 25) (Figure 1A).

After 60 minutes of ischemia, cerebral infarction was detectable in the ipsilateral hemisphere of >85% of surviving mice, predominantly in the hippocampus, cerebral cortex, and striatal regions (n = 8/9) (Figure 1B-C). Cerebral infarction was associated with prominent motor defects, manifest as a decline in movement and travel distance (Figure 1D). No TTC-measurable infarction was evident on the contralateral hemisphere (Figure 1C). In contrast, only 25% and 62.5% of surviving animals subjected to 25 (n = 1 of 4) or 45 (n = 5 of 8) minutes of ischemia, respectively, exhibited TTC-measurable cerebral infarcts. Sixty minutes of ischemia in the iCAT model generated prominent cerebral infarcts at 24 hours (mean ± standard error of the mean, 30 ± 8 mm^3; n = 8 of 9) (Figure 1B). Consistent with previous reports,[33] the extent of cerebral ischemia and infarction was highly dependent on the ambient room temperature during the surgical procedure, with infarct volumes increasing up to 1.5-fold when the room temperature was increased by 2°C. Based on these findings, subsequent studies reported in this article used a stenosis time of 60 minutes to achieve consistent stroke induction (Figure 1; supplemental Figures 1 and 2).

Cerebral perfusion monitoring predicts infarction in the iCAT stroke model

The importance of cerebral perfusion monitoring for predicting tissue salvageability and persistent microvascular hypoperfusion is well recognized.[34,35] In the iCAT stroke model, LSCI of the ipsilateral hemisphere was predictive of cortical infarction (Figure 2). Severe

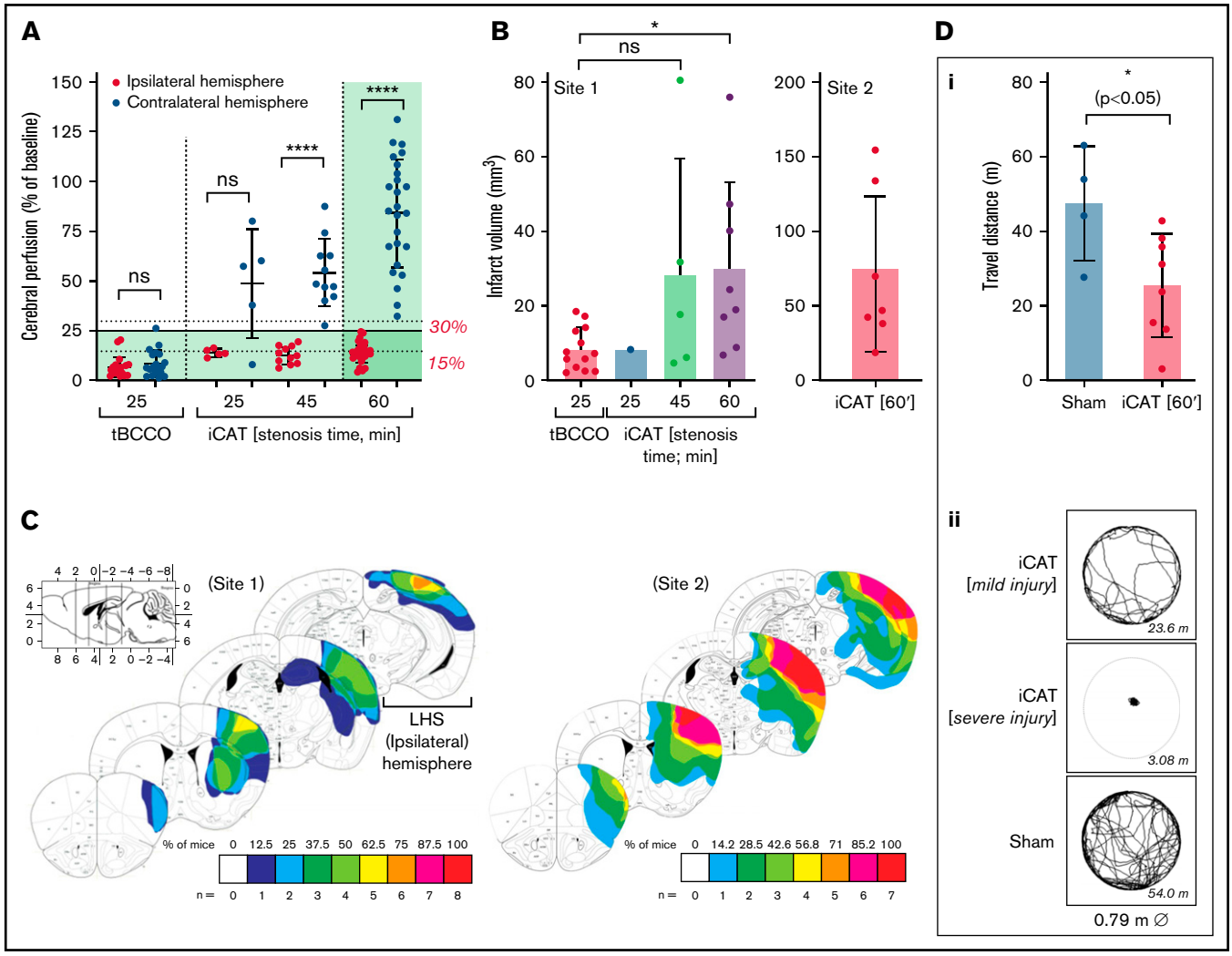

Figure 1. The iCAT stroke model causes unihemispheric infarction. C57BL/6 male mice underwent the iCAT procedure (25, 45, and 60 minutes' stenosis) or thrombotic bilateral common carotid artery occlusion (tBCCO) procedure (25 minutes). (A) Dot plot depicting the average perfusion drop (percentage of baseline) for mice in each cohort, in which the ischemic threshold is indicated by the solid gray line (25% baseline). The average cerebral perfusion of the ipsilateral (left, red symbols) and contralateral (right, blue symbols) cerebral hemispheres was assessed with LDF for the duration of the stroke induction period and presented as a percentage of baseline perfusion. Specifically, LDF readings are presented as the average cerebral perfusion immediately after bilateral occlusion until clamp removal (supplemental Figure 1Bii a-b) or immediately after stenosis application to immediately after stenosis release (supplemental Figure 1Cii; between a and b). (B-D) A subset of animals from panel A were recovered to 24 hours' postischemia induction at Site 1. Site 2 represents experiments completed at a secondary site where ambient room temperature was >2°C warmer than Site 1. (B) Infarct volume was assessed with TTC staining, with dot plots depicting infarct volumes at 24 hours in surviving animals. Data in panels A and B represent the mean ± standard deviation, analyzed to assess statistical significance using one-way analysis of variance, where $^{ns}P > .05$, $^{*}P < .05$, $^{****}P < .001$. (C) The infarct area of individual mice subjected to 60 minutes of graded stenosis at either Site 1 or 2 (quantified in panel B) was demarcated and overlaid onto a single image of the relevant brain section, with layers color-coded to reflect the number (n) of animals presenting with cerebral infarction within the denoted region (as indicated by the color key). (D) Post 24-hour recovery, functional evaluation of animals undergoing either sham or 60 minutes of iCAT-induced ischemia was conducted with open-field assessment using MouseMove[61] at Site 1. The histogram depicts quantification of travel distance in animals undergoing either sham or 60 minutes of iCAT-induced ischemia (i) or depicts travel patterns taken from representative mice for each of sham and iCAT (mild and severe injury) (ii). ns, not significant.

hypoperfusion of the ipsilateral hemisphere was predictive of mortality in 80% of cases (n = 8 of 10), whereas moderate hypoperfusion within the ipsilateral hemisphere was predictive of cerebral infarction or stroke-related mortality in 96% of cases (n = 26). Furthermore, the extent of cerebral injury in the iCAT model was predicted by the area of severely hypoperfused tissue and the degree of hypoperfusion within that area. Infarction was predicted by moderate hypoperfusion (18%-45%) over a large area of ipsilateral hemisphere (45%-68%) with 90.5% accuracy (Figure 3). In animals in which large regions of the brain (area >68%) experienced severe hypoperfusion (CBF <20%), mortality was predicted in 80% of cases (n = 12 of 15). Overall, LSCI analysis at 90 minutes' postinduction of stroke was a reliable predictor of cerebral injury in the iCAT model.

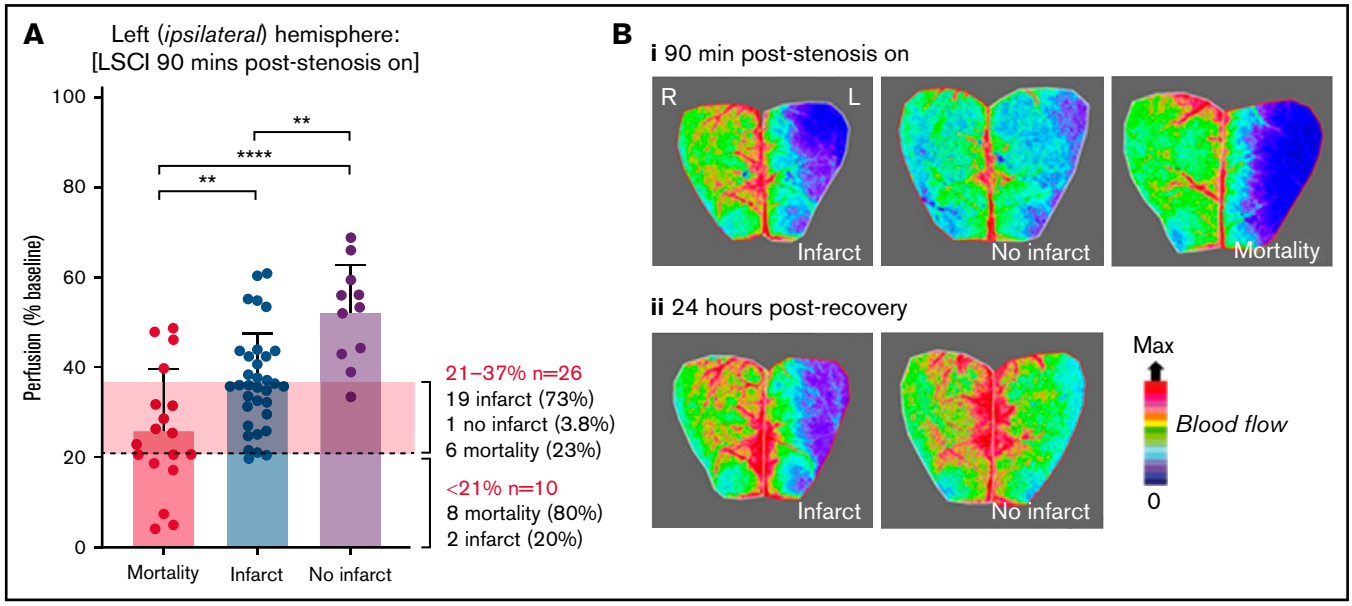

Figure 2. Cortical perfusion measurements are predictive of stroke outcomes in the iCAT model. C57BL/6 mice were subjected to the iCAT stroke model (60 minutes' ischemia), with LCSI assessed at 90 minutes' poststroke onset (stenosis on). Mice were then recovered and assessed for stroke outcomes, including mortality and presence of infarction at 24 hours. (A) Quantification of cerebral perfusion at 90 minutes, grouped according to 24-hour stroke outcome (mortality, infarct/no infarct), with data depicted as the mean ± standard deviation, with statistical significance analyzed by using an ordinary one-way analysis of variance with Šidák's multiple comparisons test, where $^{**}P < .01$, $^{****}P < .0001$. (B) LSCI examples show flux readouts of cortical cerebral perfusion in the ipsilateral (left; L) and contralateral (right; R) hemisphere at 90 minutes (i) and 24 hours (ii) after stroke onset, with a representative image taken from 1 of all 3 stroke outcome categories assessed (ie, mortality, no infarct, and infarct). Experiments were conducted at ambient temperature <21°C (Site 1).

Impact of anticoagulation on thrombolysis in the iCAT stroke model

To assess the suitability of the iCAT for testing thrombolytic therapies, we examined recanalization and associated stroke outcomes when mice were treated with rtPA alone. Our initial studies revealed that rates of recanalization achieved with rtPA in the iCAT model were low, typically occurring in <30% of treated mice. Recanalization was mostly transient, due to a high rate of rethrombosis after the initial recanalization event (Figure 4A), resulting in only 5% of treated mice exhibiting sustained recanalization. As a result, rtPA was ineffective at restoring cerebral perfusion (Figure 4C) and did not significantly reduce infarct size (Figure 5B).

The release of clot-bound thrombin after successful thrombolysis plays an important role in promoting platelet activation and fibrin generation, leading to rethrombosis.[36] We therefore investigated the impact of the direct thrombin inhibitor argatroban on rtPA-mediated recanalization and rethrombosis. As shown in Figure 4A, argatroban-treated mice with high levels of anticoagulation (~3-fold prolongation of APTT) improved the rate of rtPA-mediated recanalization from ~30% up to ~45%, with sustained recanalization achieved in 28% of mice. Where recanalization occurred, carotid artery patency improved ~2-fold compared with rtPA therapy alone (Figure 4B). However, improved carotid artery blood flow (supplemental Figure 5) failed to translate to improved cortical cerebral perfusion (Figure 4C). Moreover, increased recanalization with argatroban resulted in an increase in stroke-related mortality (from 25% to 42%). Notably, the highest mortality occurred in successfully recanalized mice (57%) (Figure 5A); the mortality rate in mice without successful recanalization was similar between the rtPA- and rtPA/argatroban–treated animals (Figures 4C and 5A).

To gain insight into the mechanism by which argatroban exacerbated cerebral injury in the iCAT stroke model, we examined the carotid blood flow traces in mice that were successfully recanalized with rtPA and argatroban therapy. We observed sudden and sustained return of carotid artery blood flow in 86% of iCAT mice that successfully recanalized with rtPA/argatroban therapy (Figure 5C). However, sudden carotid artery recanalization (Figure 5Di) was associated with persistent hypoperfusion within the ipsilateral MCA territory. Similarly, assessment of carotid artery flow and CBF revealed a paradoxical reduction in perfusion of the MCA territory upon successful recanalization (Figure 5Dii). This inverse relationship between recanalization and cortical hypoperfusion was likely to be thrombus related, rather than a vasomotor response, as sudden carotid artery mechanical recanalization with a microvascular clamp resulted in a concomitant increase in CBF (supplemental Figure 5). Impaired perfusion within the rtPA/argatroban–treated animals raised the possibility that anticoagulation was causing embolization and distal vascular obstruction.

To investigate this possibility, we developed a transillumination method that allows real-time analysis of thrombus dynamics in the carotid artery of mice.[31] Platelet-rich thrombi rapidly form at the site of electrolytic injury and are readily identified with this imaging method (Figure 6A; supplemental Figure 6). Real-time imaging of thrombolysis with rtPA confirmed transient and incomplete lysis of carotid artery thrombi, with subsequent rapid accrual of platelets onto the thrombus surface (n = 8), resulting in complete vessel

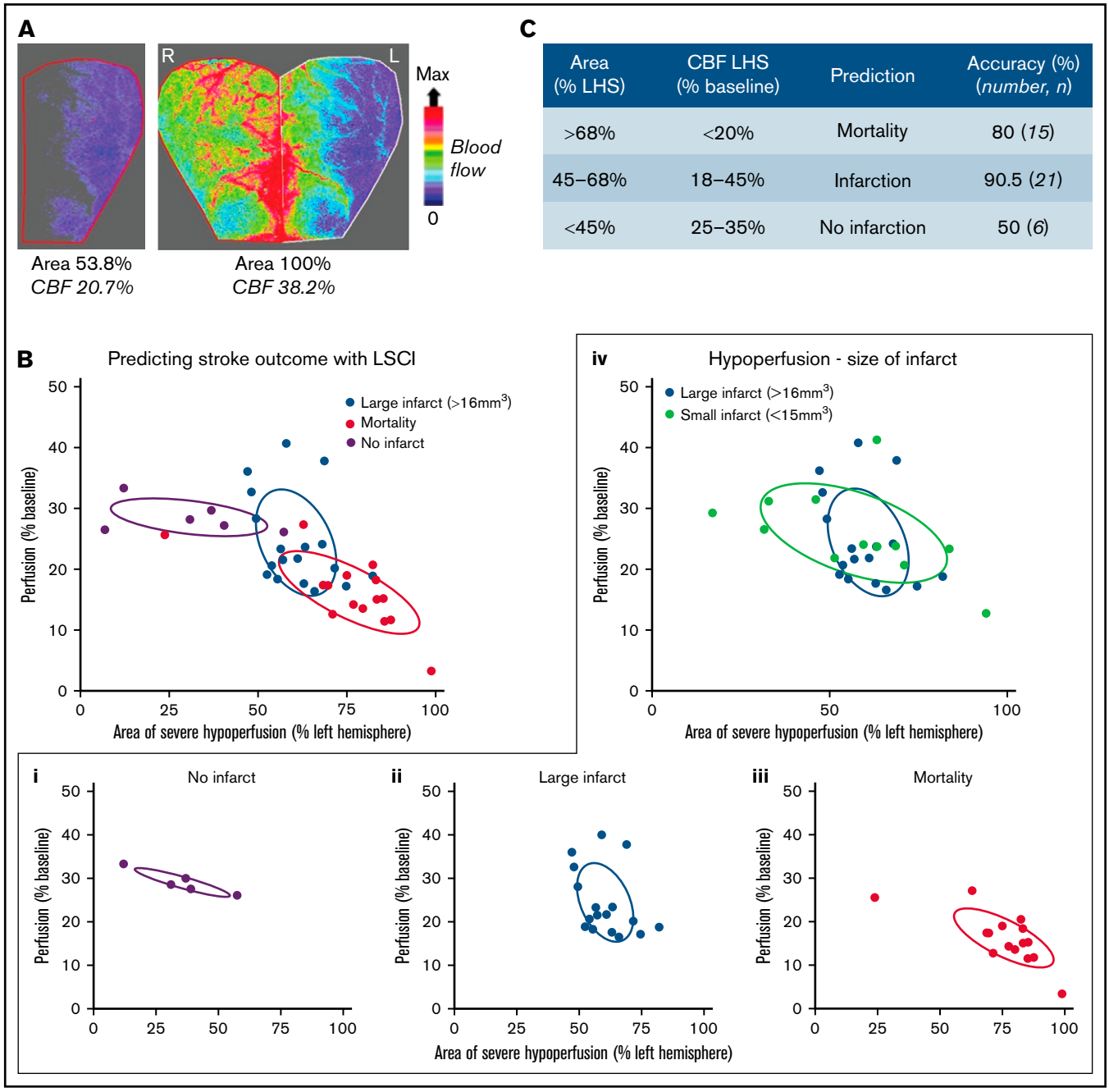

Area (% LHS)	CBF LHS (% baseline)	Prediction	Accuracy (%) (*number, n*)
>68%	<20%	Mortality	80 (*15*)
45–68%	18–45%	Infarction	90.5 (*21*)
<45%	25–35%	No infarction	50 (*6*)

Figure 3. Stroke outcome at 24 hours is predicted by cortical perfusion measurements. C57BL/6 mice were subjected to the iCAT stroke model (60 minutes' ischemia). (A) Representative flux image of the ipsilateral (L) and contralateral (R) cerebral cortex of a C57BL/6 mouse at 90 minutes' post–stroke onset, in which the left inset depicts the area of ipsilateral hemisphere with severe hypoperfusion, defined as threshold <250 flux units, as quantified using moorReview 5.0 software. (B) Scatter plots represent the calculated area of severe hypoperfusion (as assessed in panel A) correlated with the overall degree of hypoperfusion within the same region, for each individual mouse. Data were analyzed by using XLSTAT (Addinsoft, Paris, France) to highlight any correlation between the level of hypoperfusion and stroke outcomes, where mice were grouped according to their outcome at 24 hours, including no infarct (no TTC-visible infarction) (i), large infarct (infarct visible on TTC > 16 mm^3) (ii), and small infarct (infarct visible on TTC < 15 mm^3) or mortality (iii), where an individual mouse was deceased before end point. (iv) Severe and moderate hypoperfusion were classified as LSCI flux <21% of baseline and LSCI flux between 21% and 37% of baseline, respectively. (C) Tabulated summary depicting area of hypoperfusion and correlated predictive outcome, based on the analysis presented in panel B. Experiments were conducted at ambient temperature <21°C (Site 1).

reocclusion. In contrast, in the presence of argatroban, sudden recanalization was associated with the destabilization of platelet-rich thrombi from the vessel wall, leading to rapid and complete embolization (Figure 6A-B; supplemental Video 1). Subsequent assessment of the brain revealed hypoperfusion of the left cerebral MCA territory (Figure 6C). Fluorescent imaging of the brain confirmed the presence of platelet-rich thrombi occluding the MCA in rtPA/argatroban–treated mice (Figure 6D). The generation of these

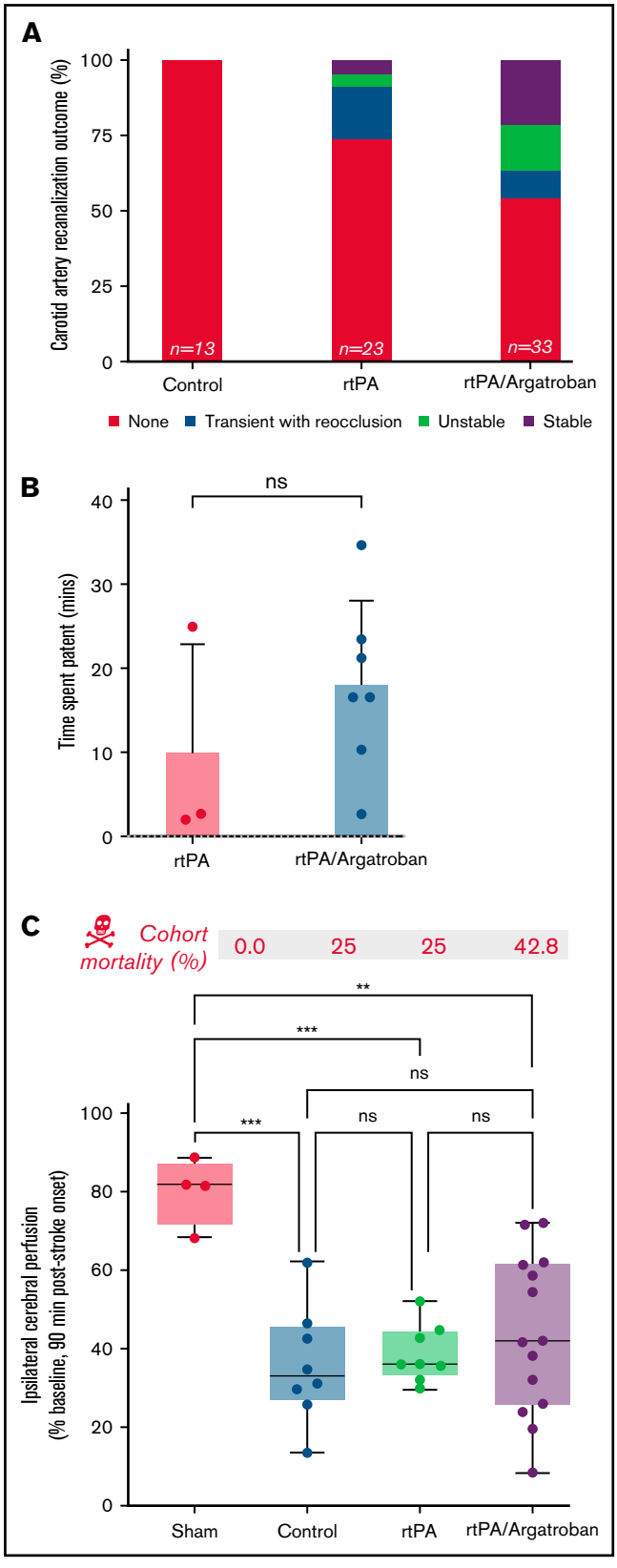

Figure 4. Combined fibrinolytic and anticoagulant therapy improves early recanalization but not cerebral perfusion. C57BL/6 mice were subjected to the iCAT stroke model (60 minutes' ischemia). Treatments were delivered IV

emboli correlated with cerebral hypoperfusion (Figure 6C-D). These studies confirm the ability of argatroban to enhance rtPA-mediated thrombolysis; however, at high levels of anticoagulation, this benefit is offset by an increased propensity to induce platelet emboli.

Discussion

Thrombolysis with rtPA remains the only pharmacologic agent for acute stroke therapy. The development of safe and effective adjunctive therapy is critical to address the shortcomings of rtPA and enhance the pharmacologic treatment of ischemic stroke. Despite clinical evidence for the importance of both large artery recanalization and microvascular cerebral reperfusion on outcome, current rodent models are not optimally designed to simultaneous assess these processes during thrombolysis. The studies outlined here show the potential utility of the iCAT stroke model in allowing assessment of adjunctive thrombolytic therapies on thrombolysis and correlate these changes with stroke outcomes (Figure 7). Our proof-of-concept studies have confirmed that argatroban can enhance thrombolysis and reduce rethrombosis and reocclusion; however, unexpectedly, at high levels of anticoagulation, this was associated with an increased propensity to produce platelet emboli, leading to distal vascular obstruction and an exacerbation of cerebral injury. The ability to examine large vessel thrombolysis in real-time and correlate this with macrovascular and microvascular changes in blood flow should provide useful new insight into the benefits and limitations of existing antithrombotic agents and assist with the future identification and optimization of alternative approaches.

Figure 4 (continued) 15 minutes after occlusion of the carotid artery (supplemental Figure 2E). Treatment dosing regimens: rtPA (10 mg/kg [1/9 mg/kg bolus/infusion over 30 minutes]); argatroban (80 μg/kg bolus; 40 μg/kg per minute infusion over 60 minutes + osmotic minipump 40 μg/kg/min infusion 23 hours). Blood flow was monitored for 60 minutes after treatment onset, and recanalization defined as measurable return of blood flow, classified as: stable (steady flow), unstable (fluctuating flow), transient with reocclusion, or none, as defined in the supplemental Methods. (A) Graph represents the percentage of animals exhibiting each specified category of blood flow, where n represents the total number of animals in each cohort. Recanalization data in the rtPA and rtPA/argatroban cohort represent pooled data from separate experimental cohorts. (B) Graph represents the amount of time vessels remain patent, quantified as a function of the area under the curve for rtPA and rtPA/argatroban cohorts. (C) A subset of animals was recovered to 24 hours for assessment of stroke outcomes (Recanalization details of this cohort alone are provided in supplemental Figure 4.) Cerebral perfusion (LSCI) was assessed at 90 minutes' post–stroke onset in sham (n = 4) and control (n = 8) animals or in animals treated with rtPA (n = 8) or rtPA/argatroban (n = 14) from a single experimental cohort. Animals that died before the 90-minute time point were not included in cerebral perfusion assessment. Quantification of ipsilateral cerebral perfusion at 90 minutes' post–stroke onset is presented in a boxplot depicting the middle 50% (box) and minimum to maximum data values obtained (whiskers), with all data points shown for clarity. Statistical analysis was performed by using an ordinary one-way analysis of variance with Tukey's multiple comparisons test, where $^{***}P < .001$, $^{**}P < .005$ and $^{ns}P > .05$. Cohort mortality Skull and crossbones ([skull and crossbones]) denote mortality rate as a percentage of animals treated (sham, n = 8; vehicle, n = 8; rtPA, n = 8; rtPA/argatroban, n = 14). ns, not significant.

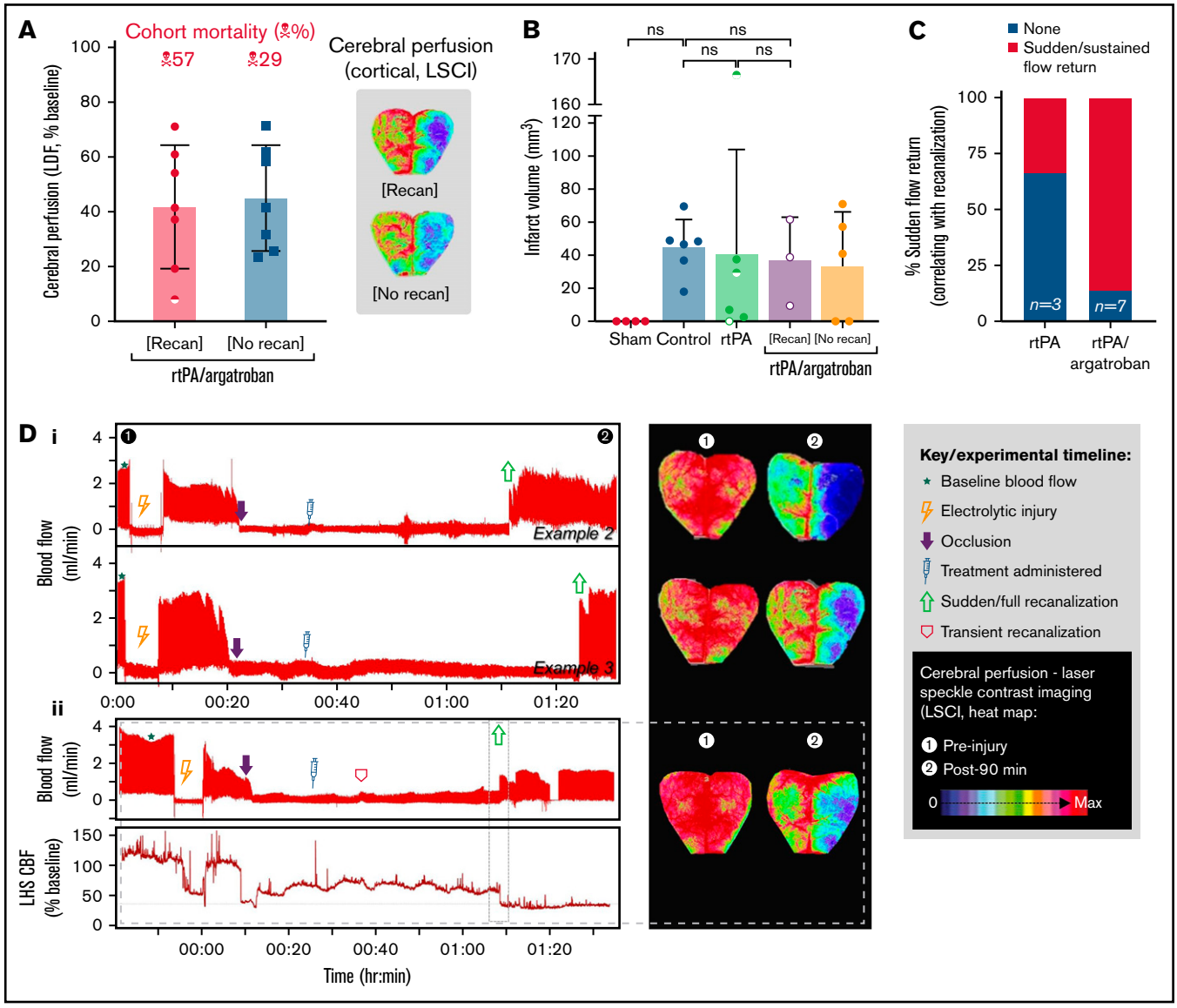

Figure 5. Combined fibrinolytic and anticoagulant therapy causes sudden recanalization and paradoxical cerebral hypoperfusion. Treatment cohorts described in Figure 4C were further analyzed for cerebral perfusion (A, LDF, left hemisphere [LHS]; LSCI, right hemisphere [RHS]), mortality (A, [skull and crossbones], expressed as %) and infarct volume (B). For mice treated with the combination of rtPA/argatroban (n = 14), outcomes were further differentiated into mice that successfully recanalized (Recan) vs those that remained occluded (No Recan). (B) Cerebral infarct was assessed with TTC staining of excised brain sections from the mouse cohorts presented in Figure 4C. Animals that died before the 24-hour point were not included in the infarct assessment. Infarct assessment was performed on experiments conducted at Site 2. In panels A and B, open circles represent animals in which embolization was observed on the flow trace, as characterized by a sudden and sustained recanalization event; half circles represent recanalization without embolization; and closed circles represent sustained occlusion. (C) Based on blood flow (LDF), the incidence of sudden and sustained recanalization events in rtPA vs rtPA/argatroban cohorts was expressed as percentage of the total number of animals in each treatment group (as indicated). (D) Examples of real-time flow traces from the iCAT procedure (i) or electrolytic injury alone (ii), and the corresponding LDF (ii) shows the sudden recanalization events, in which an abrupt return of blood flow (↑, i,ii) was observed concomitant with a reduction in LDF (ii), and sustained deficient in cerebral perfusion (LSCI heat map images, i, ii), despite full carotid recanalization. LSCI images depict CBF at baseline (pre-injury) and 90 minutes' post-carotid occlusion . ns, not significant; RBCs, red blood cells.

Murine models are the most experimentally tractable mammalian systems for the basic understanding of human biology and disease. The use of transgenic and knockout mice has been instrumental to many important basic scientific discoveries during the past 2 decades. Although murine stroke models continue to play an important role in the understanding of stroke pathogenesis, they have limitations in their ability to assess adjunctive thrombolytic therapies, including difficulties assessing recanalization in intracranial vessels, susceptibility of thrombi to endogenous fibrinolysis[15,16] or lack of thrombus for assessment, as in the intraluminal filament model of thrombotic MCAO. The development of the iCAT stroke model for the assessment of adjunctive thrombolytic agents was dependent

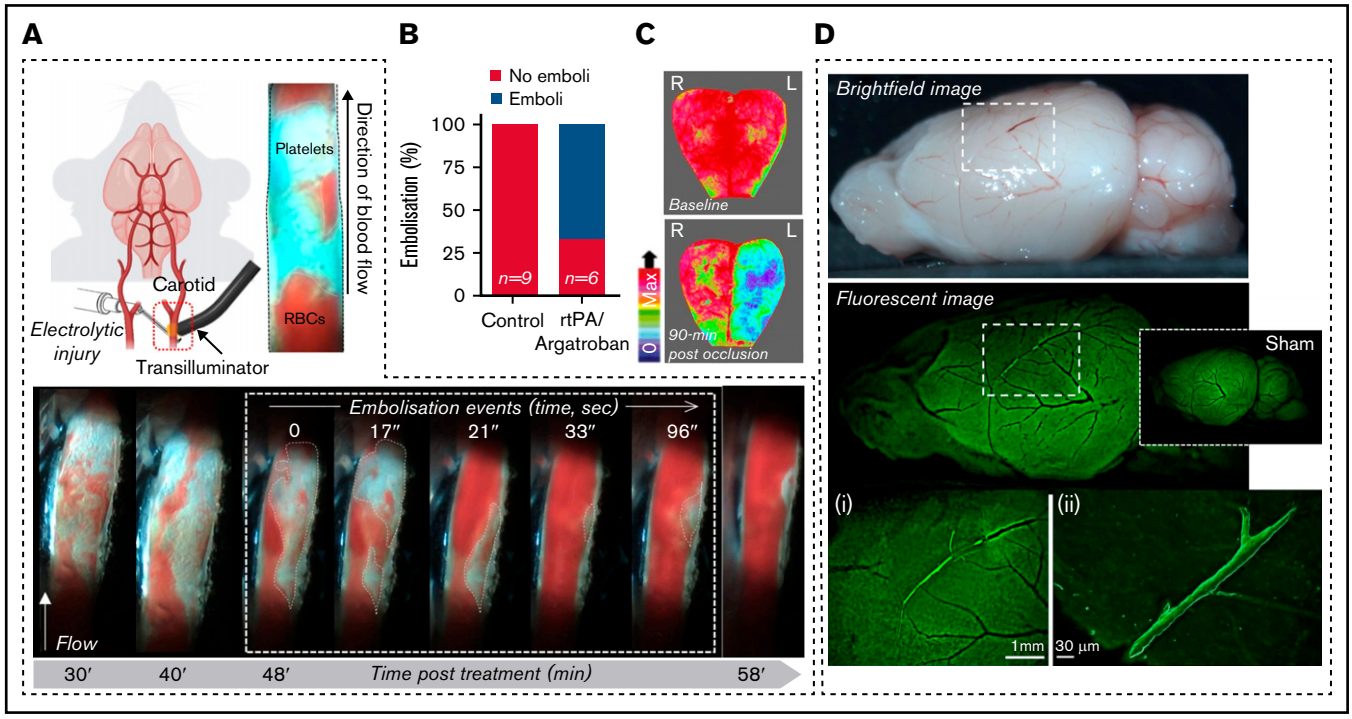

Figure 6. Combining anticoagulation and rtPA therapy induces carotid artery embolization. Electrolytic injury of the left carotid artery in C57BL/6 male mice was performed in a separate mouse cohort, with animals administered the platelet label DyLight488 before electrolytic injury (where indicated). (A) Real-time imaging of thrombolysis was conducted post-carotid occlusion, using the mouse carotid artery transilluminator, as described in the Methods. Thrombolytic therapy (vehicle control, rtPA, rtPA/argatroban) was delivered IV at 15 minutes' post-occlusion and imaging conducted for 60 minutes after treatment onset. Images presented are 1 example, from 30 to 58 minutes' posttreatment onset (platelets = white; erythrocytes = red). *Inset*: Embolization events at 48 minutes (48'00'') posttreatment onset, with platelet mass outlined by broken lines, and quantification of embolization incidence presented in panel B. (C) Global cerebral perfusion (LCSI) was assessed pre-injury (baseline) and 90 minutes' post-occlusion for the same mouse presented in panel A. The carotid artery was confirmed to be patent immediately before and immediately after collection of the LSCI reading. (D) At 90 minutes' post-occlusion, the brain from the mouse depicted in panels A and C was excised and imaged with a Nikon AZ100 Multizoom Macroscope (i, ii) and postimaging processing performed by using Nikon NIS-Element's Clarify.ai algorithm module. (ii) Confocal imaging of platelet embolus was performed by using a Leica SP8 confocal system and the three-dimensional data set acquired by using LAS X (version 3.5.7). Three-dimensional data were rendered by using Imaris version 9.8. Treatment dosing regimens: rtPA (10 mg/kg [1/9 mg/kg bolus/infusion over 30 minutes]); argatroban (80 µg/kg bolus; 40 µg/kg/min infusion over 60 minutes). Scale bars = 1 mm (panel Di); 30 = µm (panel Dii).

on the fulfillment of 4 essential criteria: (1) the development of a highly reproducible electrolytic thrombosis model that was amenable to pharmacologic thrombolysis and the assessment of adjunctive antithrombotic agents; (2) the establishment of a transilluminator imaging method that enabled real-time visualization of large vessel recanalization and reocclusion during the administration of thrombolytic and antithrombotic agents; (3) the combination of LSCI with LDF measurements of the MCA territory that allowed assessment of macrovascular and microvascular changes in cerebral perfusion during thrombolytic therapy; and (4) finally, and most importantly, the coupling of carotid artery thrombotic occlusion with controlled graded depression of ipsilateral CBF that was essential to achieve consistent cerebral hypoperfusion and reproducible focal brain injury. Fulfillment of these 4 criteria has resulted in the establishment of a highly reliable and reproducible method of arterial thrombosis and cerebral ischemia that is readily amenable to pharmacologic interventions (Figure 7).

The electrolytic injury model has not been evaluated for the study of thrombolytic therapy in mice.[28,29] Our characterization studies with the murine electrolytic model highlight that transient recanalization patterns with rtPA reflect the rethrombosis patterns observed in large animal studies and mimic aspects of gradual rtPA-mediated thrombolysis observed clinically.[37-40] In humans, arterial reocclusion after successful recanalization with rtPA is variable, ranging from 14% to 34%.[3,41] Transcranial Doppler monitoring has indicated that rethrombosis is associated with a poorer in-hospital and long-term outcome.[3] Arterial rethrombosis is more common in patients with severe ipsilateral carotid disease and in individuals with intracranial atherosclerotic disease (ICAD), occurring in up to 57.1% of cases.[42-44] Although rates of ICAD are low in Western populations (5%-10%), ICAD contributes up to 30% to 40% of ischemic strokes in Asian populations and is more prevalent in African-American and Hispanic populations.[45] It is likely that the findings from the iCAT stroke model would have greater relevance to ICAD and patients with concomitant extracranial atherosclerotic disease (tandem stenosis), in whom advanced atherosclerotic lesions are more prone to rethrombosis and vascular reocclusion after successful thrombolysis.

The inability of rtPA to induce sustained recanalization in the iCAT thrombolysis model may reflect the extensive arterial damage induced by electrolytic injury, with exposure of potent platelet activating molecules, including fibrillar collagens and tissue

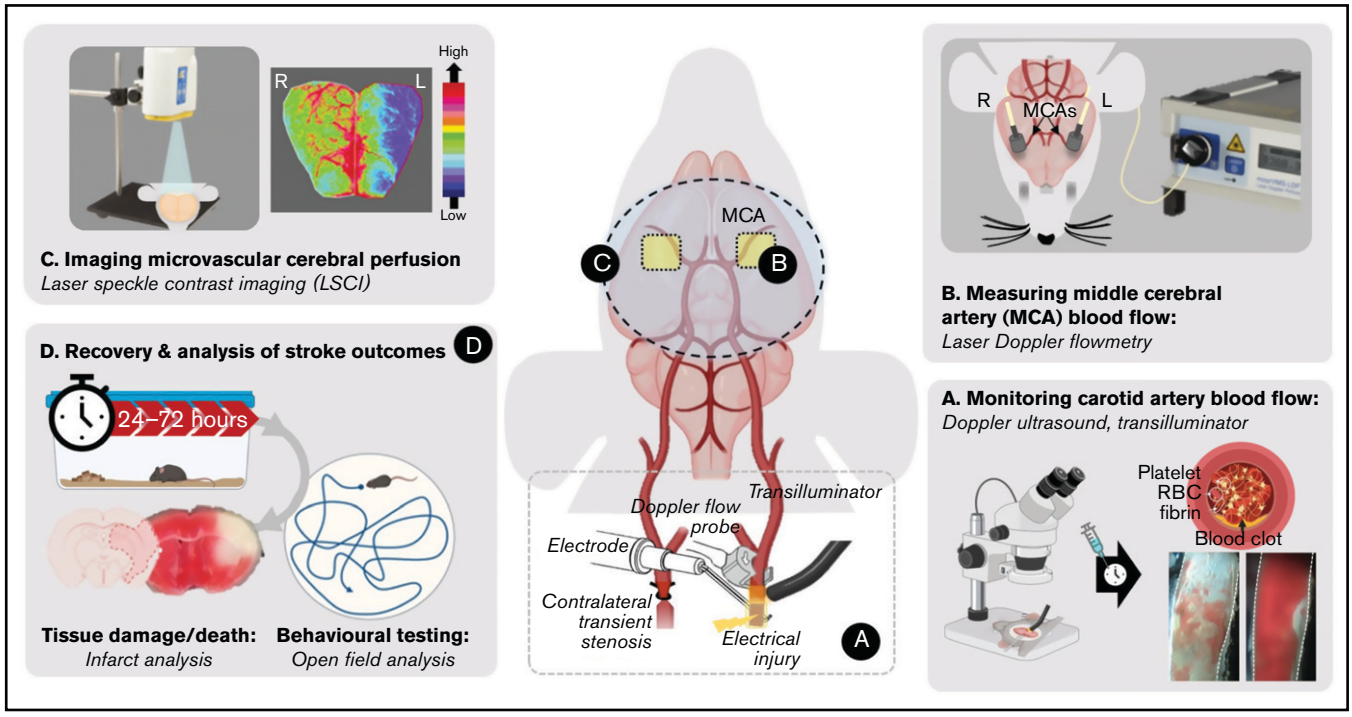

Figure 7. Schematic overview of the iCAT stroke model. (A) The iCAT model incorporates thrombotic occlusion of the CCA induced by electrolytic injury to allow for real-time monitoring of occlusion and recanalization events. (B) After thrombotic occlusion of the carotid artery, transient stenosis of the contralateral carotid artery induces ipsilateral cerebral hypoperfusion sufficient to induce infarction (<25% baseline flow), measurable with LDF over the MCA territory. Cerebral perfusion analysis with LSCI at 90 minutes' post–stroke onset is predictive of 24-hour outcome (C), including behavioral deficit, infarct progression, and mortality (D). Elements of this image were created with BioRender.com and exported under a paid subscription. RBC, red blood cell.

factor–generated thrombin.[26] Consistent with this, the direct thrombin inhibitor argatroban improved recanalization. Interestingly, in those mice surviving to 24 hours, >80% of vessels showed that initial recanalization had subsequently reoccluded 24 hours after stroke initiation, despite maintaining therapeutic levels of anticoagulation during this period. This may reflect incomplete, sustained inhibition of clot-bound thrombin, leading to persistent platelet activation and rethrombosis.[36] It is also conceivable that plasmin enhances platelet activation.[46] Nonetheless, the importance of both platelets and thrombin in this model makes it attractive for the assessment of adjunctive antithrombotic approaches.

From a practical perspective, the iCAT model shares many of the same surgical and methodologic features as the well-established intraluminal filament model MCAO. Use of the intraluminal filament MCAO model alongside the iCAT model could provide a comprehensive and complementary assessment of the neuroprotective potential of adjunct therapies. The multistep induction of carotid artery thrombosis and ischemia requires continual monitoring of carotid artery blood flow and CBF to provide insight into the relationship between recanalization and reperfusion. Consequently, the requirements of the iCAT model restrict a single operator to one iCAT stroke induction at a time, with stroke induction requiring 3 to 3.5 hours from initial anesthesia induction to recovery. Overall, in our hands, the infarct sizes, functional defects, level of reproducibility, and mortality rates between the iCAT model and MCAO model are broadly similar, with the added advantage that the iCAT model provides a wealth of data on thrombus composition and dynamics during thrombolysis, as well as concurrent temporal analysis of the effects of thrombolysis on carotid and MCA blood flow and cortical perfusion.

From a clinical standpoint, our demonstration that argatroban enhances rtPA-mediated recanalization and reduces rethrombosis in mice is consistent with the findings in humans, in whom the combination of anticoagulant and thrombolytic therapies reduces reinfarction in ST-segment elevation myocardial infarction (STEMI) patients.[47-51] Notably, rethrombosis rates in STEMI are further reduced by adding antiplatelet agents with rtPA and anticoagulants, supporting an important role for platelets in promoting rethrombosis after successful thrombolysis.[36,52] Our transilluminator intravital experiments have confirmed the potent platelet aggregation response that occurs after successful thrombolysis, leading to rapid and persistent arterial reocclusion. Full therapeutic doses of argatroban were unable to prevent this platelet build-up but, instead, led to the formation of unstable platelet thrombi that had an increased propensity to embolize. Embolization events are difficult to identify and are rarely reported in STEMI clinical trials, with most studies reporting on hemorrhagic and rethrombosis/reinfarction.[53,54] Transcranial Doppler studies on stroke patients receiving rtPA have confirmed that emboli are common in the MCA during thrombolysis, with the extent of embolization correlating well with success recanalization.[55] Currently, there is limited information on the impact of adjunctive anticoagulant agents on MCA embolization, particularly in patients with proximal atherosclerotic disease.

A critical issue for future investigation will be to determine whether rates of arterial embolization are dependent on the level of anticoagulation during thrombolysis.[56] In this context, we were surprised

that high, therapeutic levels of anticoagulation with argatroban during thrombolysis (3-fold increase in APTT above baseline) worsened cerebral perfusion and stroke outcomes in a subset of mice due to increased carotid artery embolization. It is notable that doses of argatroban that produce moderate levels of anticoagulation (APTT 1.75× or 2.25× baseline) are well tolerated clinically with rtPA and have a good safety profile, with no increased risk of symptomatic ICH or mortality.[11,57] Cerebral bleeding risk is directly related to the degree of anticoagulation, although the relationship between anticoagulant dose, recanalization, rethrombosis, and/or embolic risk remains poorly defined. Anticoagulants are particularly effective at reducing emboli from venous thrombi[58] but are less effective with thrombi that form on atherosclerotic lesions in large arteries.[59] The potential deleterious effects of arterial emboli on stroke outcomes have been previously reported in preclinical studies investigating the effects of inhibitors of the von Willebrand factor–glycoprotein Ib interaction.[60] This adhesive mechanism is critical for the initiation of platelet adhesion and aggregation at sites of arterial injury; however, in the context of thrombolysis, inhibiting this adhesion mechanism can increase arterial embolization and exacerbate cerebral injury. With a growing focus on the identification and development of anticoagulant and antiplatelet therapies with improved bleeding profiles, the insights afforded by the iCAT model may help identify the optimal combination of anticoagulant and antiplatelet agents required to facilitate large artery recanalization and microvascular blood flow, without causing excessive embolization.

Acknowledgments

The authors thank Chris Sobey for his contributions and valuable discussion regarding this work, Jim Matthews (University of Sydney) for guidance on statistical analysis of data, and Christopher Levi (UNSW), Marc Ellis (Heart Research Institute), Candice Delcourt (The George Institute for Global Health and Royal Prince Alfred Hospital), David Howells (University of Tasmania), and Pierre Mangin (Université de Strasbourg) for helpful comments regarding this work. The authors also thank the following researchers for their assistance with experimental procedures and/or technical support during this project: Jessica Toolan (Heart Research Institute), Helena Kim (La Trobe University), Yu (Joy) Yao (formerly of Monash University), Erin Nelson (formerly of Monash University), Brianna Coulter (Heart Research Institute), Lucy Thawley (Heart Research Institute), and the members of the Sydney Microscopy & Microanalysis (the University of Sydney node of Microscopy Australia). Illustrations in this manuscript were produced with the use of BioRender.com.

This work was funded by project grants from the National Health and Medical Research Council (NHMRC) of Australia (APP1044214, S.M.S. and S.P.J.; APP1120941, S.P.J.), the National Heart Foundation of Australia (Vanguard Grant ID102623, S.M.S.), the Brain Foundation, Australia (S.M.S.), and the Rebecca Cooper Medical Research Foundation (S.M.S. and J.A.A.M.). S.P.J. was the recipient of an NHMRC senior principal research fellowship (APP1079400) and current recipient of an NHMRC Investigator grant, Leadership 3 (APP1176016). S.P.J. and S.M.S. are recipients of the New South Wales government, Office of Health and Medical Research, Australia, Senior Researcher Cardiovascular Capacity Building Program grants.

Authorship

Contribution: J.A.A.M., A.J.T., S.M.S., and S.P.J. conceived and designed the study; J.A.A.M., A.J.T., S.A.S., B.R.H., I.A., A.L.S., and S.M.S. performed the experiments; J.A.A.M., A.J.T., and B.R.H. analyzed the data; J.A.A.M., A.J.T., S.M.S., and S.P.J. wrote the manuscript; and S.M.S. and S.P.J. supervised the experiments and project.

Conflict-of-interest disclosure: The authors declare no competing financial interests.

The current affiliation for A.L.S. is Walter and Eliza Hall Institute for Medical Research, Parkville, VIC, Australia.

The current affiliation for S.A.S. is CSL Limited, Bio21 Institute, Parkville, VIC, Australia.

ORCID profiles: J. A.A.M., 0000-0002-7872-9673; S.A.S., 0000-0002-1871-8972; B.R.H., 0000-0002-0432-3136; I.A., 0000-0002-5459-9093; A.L.S., 0000-0002-0637-2716; S.M.S., 0000-0003-0465-5840; S.P.J., 0000-0002-4750-1991.

Correspondence: Shaun P. Jackson, Heart Research Institute and Charles Perkins Centre, Level 3, D17, University of Sydney, Camperdown, NSW 2006, Australia; e-mail: shaun.jackson@hri.org.au.

References

1. Rha J-H, Saver JL. The impact of recanalization on ischemic stroke outcome: a meta-analysis. *Stroke.* 2007;38(3):967-973.
2. National Institute of Neurological Disorders and Stroke rtPA Stroke Study Group. Tissue plasminogen activator for acute ischemic stroke. *N Engl J Med.* 1995;333(24):1581-1588.
3. Alexandrov AV, Grotta JC. Arterial reocclusion in stroke patients treated with intravenous tissue plasminogen activator. *Neurology.* 2002;59(6):862-867.
4. Rubiera M, Alvarez-Sabín J, Ribo M, et al. Predictors of early arterial reocclusion after tissue plasminogen activator-induced recanalization in acute ischemic stroke. *Stroke.* 2005;36(7):1452-1456.
5. Saqqur M, Uchino K, Demchuk AM, et al; CLOTBUST Investigators. Site of arterial occlusion identified by transcranial Doppler predicts the response to intravenous thrombolysis for stroke. *Stroke.* 2007;38(3):948-954.
6. French JK, Edmond JJ, Gao W, White HD, Eikelboom JW. Adjunctive use of direct thrombin inhibitors in patients receiving fibrinolytic therapy for acute myocardial infarction. *Am J Cardiovasc Drugs.* 2004;4(2):107-115.
7. Domanovits H, Nikfardjam M, Janata K, et al. Restoration of coronary blood flow by single bolus injection of the GPIIb/IIIa receptor antagonist c7E3 Fab in a patient with acute myocardial infarction of recent onset. *Clin Cardiol.* 1998;21(7):525-528.

8. Rebeiz AG, Johanson P, Green CL, et al. Comparison of ST-segment resolution with combined fibrinolytic and glycoprotein IIb/IIIa inhibitor therapy versus fibrinolytic alone (data from four clinical trials). *Am J Cardiol.* 2005;95(5):611-614.

9. Ciccone A, Motto C, Abraha I, Cozzolino F, Santilli I. Glycoprotein IIb-IIIa inhibitors for acute ischaemic stroke. *Cochrane Database Syst Rev.* 2014;(3):CD005208.

10. Zinkstok SM, Beenen LF, Majoie CB, Marquering HA, de Haan RJ, Roos YB. Early deterioration after thrombolysis plus aspirin in acute stroke: a post hoc analysis of the Antiplatelet Therapy in Combination with Recombinant t-PA Thrombolysis in Ischemic Stroke trial. *Stroke.* 2014;45(10): 3080-3082.

11. Barreto AD, Ford GA, Shen L, et al; ARTSS-2 Investigators. Randomized, multicenter trial of ARTSS-2 (Argatroban with recombinant tissue plasminogen activator for acute stroke). *Stroke.* 2017;48(6):1608-1616.

12. Morris DC, Zhang L, Zhang ZG, et al. Extension of the therapeutic window for recombinant tissue plasminogen activator with argatroban in a rat model of embolic stroke. *Stroke.* 2001;32(11):2635-2640.

13. Kawai H, Yuki S, Sugimoto J, Tamao Y. Effects of a thrombin inhibitor, argatroban, on ischemic brain damage in the rat distal middle cerebral artery occlusion model. *J Pharmacol Exp Ther.* 1996;278(2):780-785.

14. Jang IK, Gold HK, Leinbach RC, Fallon JT, Collen D. *In vivo* thrombin inhibition enhances and sustains arterial recanalization with recombinant tissue-type plasminogen activator. *Circ Res.* 1990;67(6):1552-1561.

15. Ansar S, Chatzikonstantinou E, Wistuba-Schier A, et al. Characterization of a new model of thromboembolic stroke in C57 black/6J mice. *Transl Stroke Res.* 2014;5(4):526-533.

16. Orset C, Macrez R, Young AR, et al. Mouse model of in situ thromboembolic stroke and reperfusion. *Stroke.* 2007;38(10):2771-2778.

17. Morris GP, Wright AL, Tan RP, Gladbach A, Ittner LM, Vissel B. A comparative study of variables influencing ischemic injury in the Longa and Koizumi methods of intraluminal filament middle cerebral artery occlusion in mice. *PLoS One.* 2016;11(2):e0148503.

18. Zhang Z, Chopp M, Zhang RL, Goussev A. A mouse model of embolic focal cerebral ischemia. *J Cereb Blood Flow Metab.* 1997;17(10): 1081-1088.

19. Tomkins AJ, Schleicher N, Murtha L, et al. Platelet rich clots are resistant to lysis by thrombolytic therapy in a rat model of embolic stroke. *Exp Transl Stroke Med.* 2015;7(1):2.

20. Atochin DN, Murciano JC, Gürsoy-Ozdemir Y, et al. Mouse model of microembolic stroke and reperfusion. *Stroke.* 2004;35(9):2177-2182.

21. Ren M, Lin ZJ, Qian H, et al. Embolic middle cerebral artery occlusion model using thrombin and fibrinogen composed clots in rat. *J Neurosci Methods.* 2012;211(2):296-304.

22. Labat-gest V, Tomasi S. Photothrombotic ischemia: a minimally invasive and reproducible photochemical cortical lesion model for mouse stroke studies. *J Vis Exp.* 2013;76(76):e50370.

23. Syeara N, Alamri FF, Jayaraman S, et al. Motor deficit in the mouse ferric chloride-induced distal middle cerebral artery occlusion model of stroke. *Behav Brain Res.* 2020;380:112418.

24. Sommer CJ. Ischemic stroke: experimental models and reality. *Acta Neuropathol.* 2017;133(2):245-261.

25. *National Health and Medical Research Council. Australian Code for the Care and Use of Animals for Scientific Purposes*. 8th ed. Canberra: National Health and Medical Research Council; 2013.

26. Sturgeon SA, Jones C, Angus JA, Wright CE. Adaptation of the Folts and electrolytic methods of arterial thrombosis for the study of anti-thrombotic molecules in small animals. *J Pharmacol Toxicol Methods.* 2006;53(1):20-29.

27. Mangin P, Yap CL, Nonne C, et al. Thrombin overcomes the thrombosis defect associated with platelet GPVI/FcRgamma deficiency. *Blood.* 2006; 107(11):4346-4353.

28. Schoenwaelder SM, Darbousset R, Cranmer SL, et al. 14-3-3ζ regulates the mitochondrial respiratory reserve linked to platelet phosphatidylserine exposure and procoagulant function [published correction appears in *Nat Commun*. 2017;8:16125]. *Nat Commun.* 2016;7(1):12862.

29. Guarini S. A highly reproducible model of arterial thrombosis in rats. *J Pharmacol Toxicol Methods.* 1996;35(2):101-105.

30. Samson AL, Nevin ST, Medcalf RL. Low molecular weight contaminants in commercial preparations of plasmin and t-PA activate neurons. *J Thromb Haemost.* 2008;6(12):2218-2220.

31. Jirousková M, Chereshnev I, Väänänen H, Degen JL, Coller BS. Antibody blockade or mutation of the fibrinogen gamma-chain C-terminus is more effective in inhibiting murine arterial thrombus formation than complete absence of fibrinogen. *Blood.* 2004;103(6):1995-2002.

32. Stockmans F, Stassen JM, Vermylen J, Hoylaerts MF, Nyström A. A technique to investigate mural thrombus formation in small arteries and veins: I. Comparative morphometric and histological analysis. *Ann Plast Surg.* 1997;38(1):56-62.

33. Krieger DW, Yenari MA. Therapeutic hypothermia for acute ischemic stroke: what do laboratory studies teach us? *Stroke.* 2004;35(6):1482-1489.

34. Bouts MJ, Tiebosch IA, van der Toorn A, Viergever MA, Wu O, Dijkhuizen RM. Early identification of potentially salvageable tissue with MRI-based predictive algorithms after experimental ischemic stroke. *J Cereb Blood Flow Metab.* 2013;33(7):1075-1082.

35. Cho T-H, Nighoghossian N, Mikkelsen IK, et al. Reperfusion within 6 hours outperforms recanalization in predicting penumbra salvage, lesion growth, final infarct, and clinical outcome. *Stroke.* 2015;46(6):1582-1589.

36. Weitz JI, Leslie B, Hudoba M. Thrombin binds to soluble fibrin degradation products where it is protected from inhibition by heparin-antithrombin but susceptible to inactivation by antithrombin-independent inhibitors. *Circulation.* 1998;97(6):544-552.

37. Jackson CV, Crowe VG, Craft TJ, et al. Thrombolytic activity of a novel plasminogen activator, LY210825, compared with recombinant tissue-type plasminogen activator in a canine model of coronary artery thrombosis. *Circulation.* 1990;82(3):930-940.

38. Hong TT, Huang J, Lucchesi BR. Effect of thrombolysis on myocardial injury: recombinant tissue plasminogen activator vs. alfimeprase. *Am J Physiol Heart Circ Physiol.* 2006;290(3):H959-H967.

39. McCabe C, Arroja MM, Reid E, Macrae IM. Animal models of ischaemic stroke and characterisation of the ischaemic penumbra. *Neuropharmacology.* 2018;134(Pt B):169-177.

40. Alexandrov AV, Burgin WS, Demchuk AM, El-Mitwalli A, Grotta JC. Speed of intracranial clot lysis with intravenous tissue plasminogen activator therapy: sonographic classification and short-term improvement. *Circulation.* 2001;103(24):2897-2902.

41. Saqqur M, Molina CA, Salam A, et al; CLOTBUST Investigators. Clinical deterioration after intravenous recombinant tissue plasminogen activator treatment: a multicenter transcranial Doppler study. *Stroke.* 2007;38(1):69-74.

42. Kang D-H, Kim Y-W, Hwang Y-H, Park S-P, Kim Y-S, Baik SK. Instant reocclusion following mechanical thrombectomy of in situ thromboocclusion and the role of low-dose intra-arterial tirofiban. *Cerebrovasc Dis.* 2014;37(5):350-355.

43. Mosimann PJ, Kaesmacher J, Gautschi D, et al. Predictors of unexpected early reocclusion after successful mechanical thrombectomy in acute ischemic stroke patients. *Stroke.* 2018;49(11):2643-2651.

44. Baek J-H, Kim BM, Heo JH, Kim DJ, Nam HS, Kim YD. Outcomes of endovascular treatment for acute intracranial atherosclerosis-related large vessel occlusion. *Stroke.* 2018;49(11):2699-2705.

45. Campbell BCV, De Silva DA, Macleod MR, et al. Ischaemic stroke. *Nat Rev Dis Primers.* 2019;5(1):70.

46. Quinton TM, Kim S, Derian CK, Jin J, Kunapuli SP. Plasmin-mediated activation of platelets occurs by cleavage of protease-activated receptor 4. *J Biol Chem.* 2004;279(18):18434-18439.

47. Antithrombotic Trialists' Collaboration. Collaborative meta-analysis of randomised trials of antiplatelet therapy for prevention of death, myocardial infarction, and stroke in high risk patients. *BMJ.* 2002;324(7329):71-86.

48. Lincoff AM, Califf RM, Topol EJ. Platelet glycoprotein IIb/IIIa receptor blockade in coronary artery disease. *J Am Coll Cardiol.* 2000;35(5): 1103-1115.

49. Granada JF, Kleiman NS. Therapeutic use of intravenous eptifibatide in patients undergoing percutaneous coronary intervention: acute coronary syndromes and elective stenting. *Am J Cardiovasc Drugs.* 2004;4(1):31-41.

50. Dai Y, Ge J. Clinical use of aspirin in treatment and prevention of cardiovascular disease. *Thrombosis.* 2012;2012:245037.

51. Roffi M, Chew DP, Mukherjee D, et al. Platelet glycoprotein IIb/IIIa inhibition in acute coronary syndromes. Gradient of benefit related to the revascularization strategy. *Eur Heart J.* 2002;23(18):1441-1448.

52. Owen J, Friedman KD, Grossman BA, Wilkins C, Berke AD, Powers ER. Thrombolytic therapy with tissue plasminogen activator or streptokinase induces transient thrombin activity. *Blood.* 1988;72(2):616-620.

53. Jang I-K, Brown DFM, Giugliano RP, et al; the MINT Investigators. A multicenter, randomized study of argatroban versus heparin as adjunct to tissue plasminogen activator (TPA) in acute myocardial infarction: myocardial infarction with novastan and TPA (MINT) study. *J Am Coll Cardiol.* 1999;33(7):1879-1885.

54. Allan M, Zachariah G, Kordzadeh A, Umachandran V. An uncommon complication of acute stroke thrombolysis. *BMJ Case Rep.* 2014;2014: bcr2013202054.

55. Alexandrov AV, Demchuk AM, Felberg RA, Grotta JC, Krieger DW. Intracranial clot dissolution is associated with embolic signals on transcranial Doppler. *J Neuroimaging.* 2000;10(1):27-32.

56. Shoeb M, Fang MC. Assessing bleeding risk in patients taking anticoagulants. *J Thromb Thrombolysis.* 2013;35(3):312-319.

57. Barreto AD, Alexandrov AV. Adjunctive and alternative approaches to current reperfusion therapy. *Stroke.* 2012;43(2):591-598.

58. Toth PP. Considerations for long-term anticoagulant therapy in patients with venous thromboembolism in the novel oral anticoagulant era. *Vasc Health Risk Manag.* 2016;12:23-34.

59. Sharma R, Kumar P, Prashanth SP, Belagali Y. Dual antiplatelet therapy in coronary artery disease. *Cardiol Ther.* 2020;9(2):349-361.

60. Le Behot A, Gauberti M, Martinez De Lizarrondo S, et al. GpIbα-VWF blockade restores vessel patency by dissolving platelet aggregates formed under very high shear rate in mice. *Blood.* 2014;123(21):3354-3363.

61. Samson AL, Ju L, Ah Kim H, et al. MouseMove: an open source program for semi-automated analysis of movement and cognitive testing in rodents. *Sci Rep.* 2015;5(1):16171.